Oxidation of archaeal peroxiredoxin involves a hypervalent sulfur intermediate

Tsutomu Nakamura[†‡], Takahiko Yamamoto[§¶], Manabu Abe[§‖], Hiroyoshi Matsumura[§], Yoshihisa Hagihara[†], Tadashi Goto[§], Takafumi Yamaguchi[§], and Tsuyoshi Inoue[‡§]

[†]National Institute of Advanced Industrial Science and Technology, Ikeda, Osaka 563-8577, Japan; and [§]Department of Applied Chemistry, Graduate School of Engineering, Osaka University, Suita, Osaka 565-0871, Japan

Edited by Brian W. Matthews, University of Oregon, Eugene, OR, and approved February 15, 2008 (received for review October 16, 2007)

The oxidation of thiol groups in proteins is a common event in biochemical processes involving disulfide bond formation and in response to an increased level of reactive oxygen species. It has been widely accepted that the oxidation of a cysteine side chain is initiated by the formation of cysteine sulfenic acid (Cys-SOH). Here, we demonstrate a mechanism of thiol oxidation through a hypervalent sulfur intermediate by presenting crystallographic evidence from an archaeal peroxiredoxin (Prx), the thioredoxin peroxidase from *Aeropyrum pernix* K1 (ApTPx). The reaction of Prx, which is the reduction of a peroxide, depends on the redox active cysteine side chains. Oxidation by hydrogen peroxide converted the active site peroxidatic Cys-50 of ApTPx to a cysteine sulfenic acid derivative, followed by further oxidation to cysteine sulfinic and sulfonic acids. The crystal structure of the cysteine sulfenic acid derivative was refined to 1.77 Å resolution with R_{cryst} and R_{free} values of 18.8% and 22.0%, respectively. The refined structure, together with quantum chemical calculations, revealed that the sulfenic acid derivative is a type of sulfurane, a hypervalent sulfur compound, and that the S^{γ} atom is covalently linked to the $N^{\delta 1}$ atom of the neighboring His-42. The reaction mechanism is revealed by the hydrogen bond network around the peroxidatic cysteine and the motion of the flexible loop covering the active site and by quantum chemical calculations. This study provides evidence that a hypervalent sulfur compound occupies an important position in biochemical processes.

thioredoxin peroxidase | sulfurane | peroxidatic cysteine | *Aeropyrum pernix* K1 | thiol oxidation

Hypervalent compounds (1) have attracted considerable attention in many fields of chemistry, because they possess unusual structures and reactivities, brought about by their unique bond, a three-center-four-electron bond. For example, sulfurane, a hypervalent sulfur compound containing a trigonal bipyramidal structure with four ligands, is effective for dehydration reactions, the synthesis of epoxides and nitriles, and certain alkylation reactions (2). In comparison with the attention these receive in the synthetic organic literature, hypervalent compounds from natural sources have not been emphasized to date. In this article, the existence of a hypervalent sulfur compound (a sulfurane derivative) from biological sources, which occurs during thiol oxidation in a protein, is demonstrated. We present x-ray crystallographic evidence for the sulfurane derivative of an archaeal peroxiredoxin (Prx), the thioredoxin peroxidase from *Aeropyrum pernix* K1 (ApTPx).

Prxs are thiol-dependent peroxidases that reduce hydrogen peroxide and alkyl peroxides to water and the corresponding alcohols, respectively (3–5). In addition to antioxidant functions, Prxs maintain the intracellular level of hydrogen peroxide that affects signal mediators such as protein tyrosine phosphatase (6) and the lipid phosphatase PTEN (7) through its self-inactivation mechanism (8). These two distinct functions make Prx a switching molecule that regulates the cellular H_2O_2 level. In general, the oxidation of a cysteine side chain of protein is initiated by the formation of cysteine sulfenic acid (Cys-SOH) (9–12). The same oxidation mechanism has been reported also for the oxidation process of Prx proteins. Prx contains a redox active peroxidatic cysteine (C_p) residue in its N-terminal region. It has been reported that the first step of the reaction of Prx is the formation of the single-oxidation intermediate, cysteine sulfenic acid (C_p-SOH). Cysteine sulfenic acid is prone to further oxidation in aqueous solution, leading to a self-inactivation process by overoxidation to form cysteine sulfinic acid (C_p-SO_2H) and cysteine sulfonic acid (C_p-SO_3H). A recycling process is known in eukaryotic 2-Cys Prxs, in which C_p-SO_2H is converted to C_p-SOH by an ATP-dependent reduction catalyzed by sulfiredoxin (13). In the peroxidase process of Prx, the single-oxidation intermediate is followed by disulfide linkage formation or reaction with a cellular reductant, depending on the subtype of the Prx [typical 2-Cys, atypical 2-Cys, or 1-Cys Prxs (3)]. For the peroxidase process, a protective mechanism is likely to act against the overoxidation of the C_p residue. Besides the tertiary structures of the Prxs in the reduced and disulfide states, several structures have been solved for the sulfenic acid (14, 15), sulfinic acid (16), and sulfonic acid (17, 18) forms. To date, however, there have been no extensive structural determination studies covering all redox states of the same Prx. Such information would provide the key to elucidate the architecture of the thiol redox process in proteins.

The crystal structures of ApTPx have been reported for the reduced (19) and sulfonic acid (18) forms. Because Jeon and Ishikawa (20) suggested that ApTPx is a typical 2-Cys Prx with peroxidatic Cys-50 and resolving Cys-213, we have performed crystallographic studies on the mutant C207S of ApTPx (19, 21), in which the other cysteine residue (Cys-207) was replaced to avoid unfavorable thiol modification. In this article, we present crystal structures of ApTPx in multiple oxidation states and describe the structural changes on oxidation. Here, we also present a mechanism of thiol oxidation through a hypervalent sulfur intermediate.

Results and Discussion

Crystal Structures of Oxidized ApTPx. The asymmetric unit of the ApTPx crystal contains 10 molecules forming a decameric ring

Author contributions: T.N., T. Yamamoto, and M.A. contributed equally to this work; T.N. and T.I. designed research; T.N., T. Yamamoto, M.A., H.M., Y.H., T.G., T. Yamaguchi, and T.I. performed research; and T.N. wrote the paper.

The authors declare no conflict of interest.

This article is a PNAS Direct Submission.

Data deposition: The atomic coordinates and structure factors of the preoxidation, hypervalent sulfur, sulfinic acid, and sulfenic acid forms have been deposited in the Protein Data Bank, www.pdb.org (PDB ID codes 2E2G, 2ZCT, 2E2M, and 2NVL, respectively).

[‡]To whom correspondence may be addressed. E-mail: nakamura-t@aist.go.jp or inouet@chem.eng.osaka-u.ac.jp.

[¶]Present address: Shionogi & Co, Ltd., Osaka 553-0002, Japan.

[‖]Present address: Department of Chemistry, Graduate School of Science, Hiroshima University, Higashi-Hiroshima, Hiroshima 739-8526, Japan

This article contains supporting information online at www.pnas.org/cgi/content/full/0709822105/DCSupplemental.

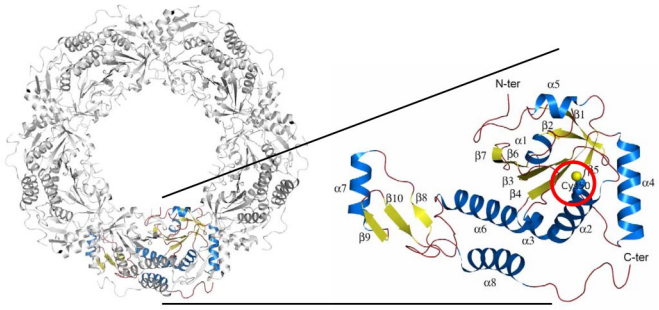

Fig. 1. Whole structure and side chain of the peroxidatic cysteine. The decameric (*Left*) and monomeric structures (*Right*) of ApTPx are shown. The peroxidatic cysteine (C_p50) is indicated by a red circle.

(Fig. 1). The C_p50 is on the N-terminal end of α-helix 2 (Fig. 1). We observed four different structures of ApTPx associated with the H_2O_2-mediated oxidation, in addition to the previously reported reduced form (19): preoxidation, single-oxidation, sulfinic acid, and sulfonic acid forms (supporting information (SI) Fig. S1). The crystallization and refinement statistics of these forms are shown in Table S1. The single-oxidation form, which was refined to 1.77 Å resolution with R_{cryst} and R_{free} values of 18.8% and 22.0%, respectively, represents the characteristic structure as follows. In this form, an extra oxygen atom bonds covalently to the S^{γ} atom of C_p50. In addition, the S^{γ} atom is situated near $N^{\delta 1}$ of His-42. The distance between these atoms is so close (2.2 Å) that they are considered to form a covalent bond rather than a hydrogen bond (Fig. 2*a*). The bond angle

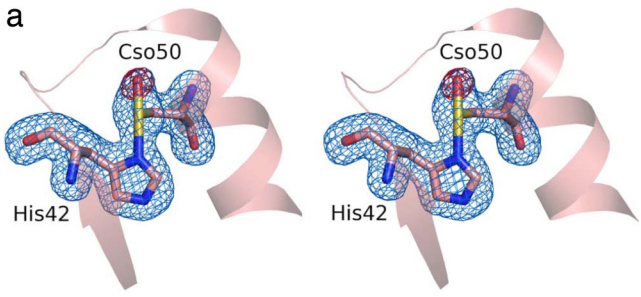

b

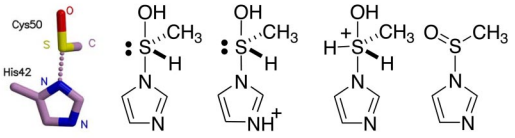

	Observed	Model 1	Model 2	Model 3	Model 4
Angle (O-S-C, °)	81.3 ± 2.8	91.5	93.7	87.8	106.55
Angle (O-S-N, °)	170.2 ± 4.5	170.3	172.4	174.1	109.9
Angle (N-S-C, °)	99.9 ± 3.7	88.2	89	98	95.29
Distance (O-S, Å)	1.72 ± 0.01	1.8	1.68	1.7	1.49
Distance (S-N, Å)	2.21 ± 0.13	1.97	2.39	1.77	1.77

Fig. 2. Structure of the hypervalent sulfur intermediate. (*a*) A stereo diagram of ApTPx around the peroxidatic cysteine in the hypervalent sulfur form. The blue electron density indicates the σ_A-weighted $|F_o| - |F_c|$ electron density map at the 4.0 σ level, where the two amino acid residues (His-42 and Cso-50) were removed from the structure factor calculation. The red density indicates the σ_A-weighted $|F_o| - |F_c|$ map at the 3.5-σ level, where the oxygen atom of the side chain of Cso-50 was removed from the structure factor calculation. Cso represents the C_p residue in the hypervalent sulfur form. (*b*) List of bond angles and distances. Values for the crystal structure (shown on the left) are the average ± SD of the 10 subunits. The columns of models 1–4 show the calculated values of each model.

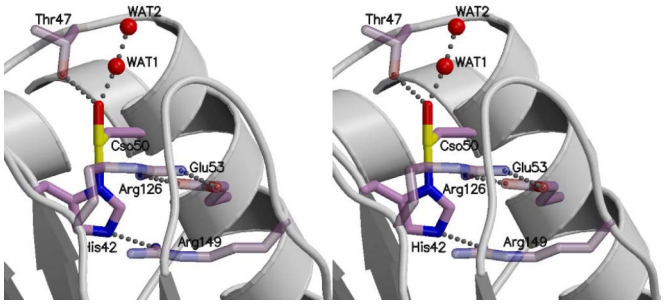

Fig. 3. Interaction of the hypervalent intermediate with surrounding residues.

formed around the S^{γ} atom shows a characteristic feature where the $N^{\delta 1}$, S^{γ}, and O^{δ} atoms are aligned linearly and the C^{β} atom of C_p50 bonds to the S^{γ} from the perpendicular direction. This feature is common in all of the 10 subunits; the observed bond angles and distances are listed in Fig. 2*b* and Fig. S2.

Models for the Reaction Intermediate. To know the chemical structure of the single-oxidation form, we performed quantum chemical calculations of possible models and searched for the compound that best fits the observed structure by x-ray crystallography. The model (hydroxy-imidazolyl-λ^4-sulfanyl)methane, a hypervalent sulfur compound (sulfurane derivative), was found to be in good agreement with the observed structure (Fig. 2*b*, models 1 and 2). The crystal structure is considered to represent a mixture of sulfurane derivatives with either a neutral or protonated imidazole moiety.

The calculations for other chemical forms did not fit the observed structure as described below. Although three ligands (nitrogen, oxygen, and carbon atoms) of the sulfurane model are evident from the crystal structure, the lone pair and hydrogen ligand are not visible in the x-ray crystallography at the normal resolution. To confirm the existence of the lone pair and hydrogen ligand, we simulated the atomic coordinates of the modified form of the sulfurane derivative and compared these with the observed structures. When the hydrogen atom was removed from the model compound, the interaction between the sulfur and nitrogen atoms disappeared, regardless of whether the imidazole moiety was protonated or not (data not shown). Next, we assumed the model in which another hydrogen ligand was added so that the sulfur atom had five ligands. When the imidazole moiety was neutral, the distance between the sulfur and the nitrogen atoms was calculated to be 1.77 Å (Fig. 2*b*, model 3), which was significantly shorter than the observed length. Protonation of the imidazole moiety in model 3 (Fig. 2*b*) resulted in it splitting into two parts because of a lack of interaction between the sulfur and nitrogen atoms (data not shown).

As an alternative model for a compound with a sulfur atom ligated with nitrogen, carbon, and oxygen atoms, we assumed a sulfinamide, which has been found in other cysteine-containing proteins and peptides (22, 23). We calculated the optimized structure of the model imidazoylmethanesulfinamide (Fig. 2*b*, model 4). The calculated structure of the sulfinamide model was far from that of the observed structure: the model did not have a linear alignment of oxygen, sulfur, and nitrogen atoms. For all of the protonated derivatives of the sulfinamide (*N*-protonated imidazoylmethanesulfinamide, *S*-protonated imidazoylmethanesulfinamide, and *N*,*S*-diprotonated imidazoylmethanesulfinamide), the alignment of the three atoms was not linear: the angles (O–S–N) were <115° (data not shown). Thus, the possibility of the sulfinamide derivative being considered as the oxidized intermediate of ApTPx was excluded.

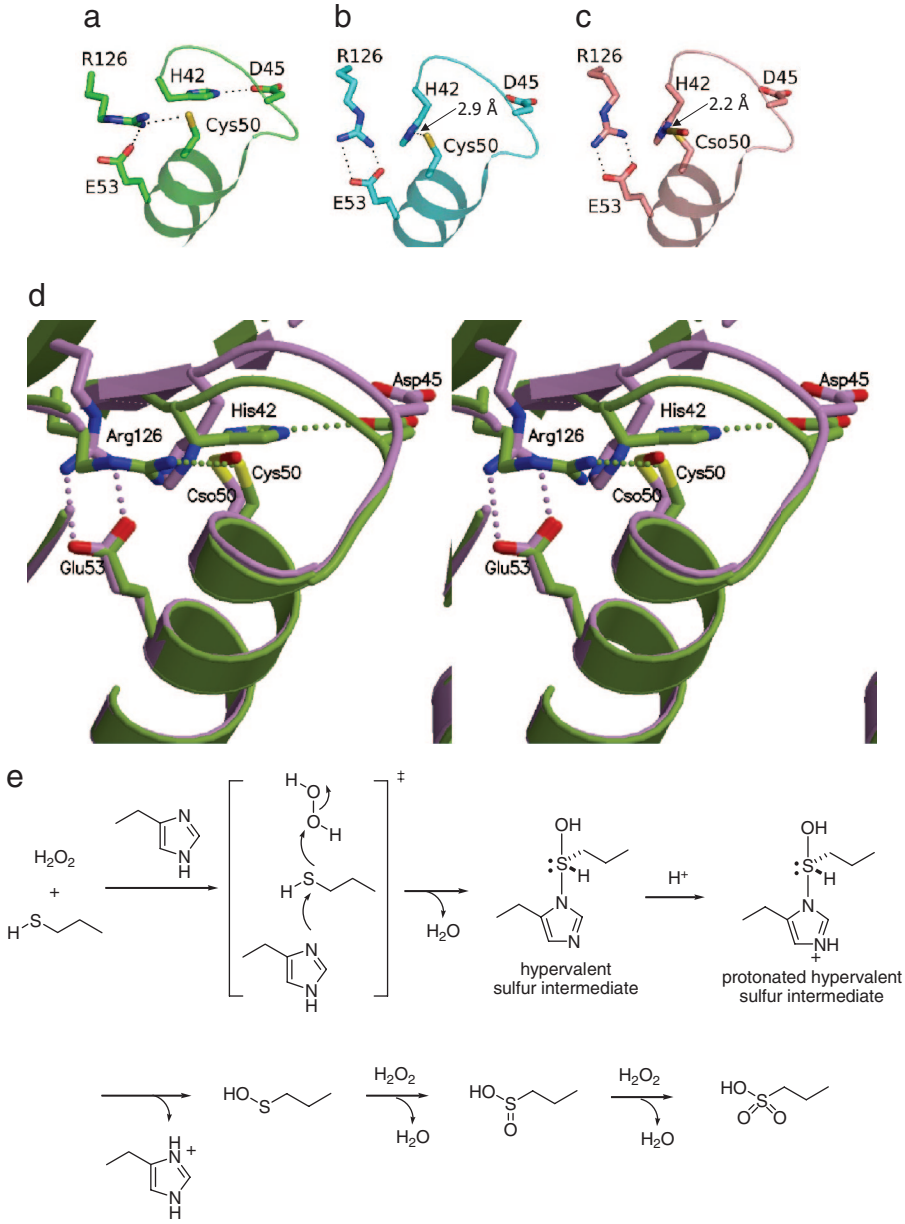

Fig. 4. Structural change and putative reaction scheme of ApTPx. (*a–c*) Close-ups around the peroxidatic cysteine residues of the reduced, preoxidation, and hypervalent sulfur forms, respectively. (*d*) Superimposition of the reduced (green) and hypervalent sulfur (purple) forms. Proposed reaction scheme of ApTPx is shown in *e*. Cso represents the C_p residue in the hypervalent sulfur form.

These results confirm that the crystal structure of ApTPx in the single-oxidation form represents the sulfurane derivative, a hypervalent sulfur compound containing a trigonal bipyramidal structure with four ligands. These crystallographic and theoretical studies show evidence of a hypervalent sulfur compound in biomolecules.

Interaction of the Hypervalent Intermediate with Neighboring Residues. The sulfurane moiety of the hypervalent sulfur intermediate is stabilized by interactions with neighboring residues (Fig. 3), confirming the validity of this intermediate. In the sulfurane intermediate, the $N^{\varepsilon 2}$ atom of His-42 is in contact with Arg-149, which seems to be involved in the protonation process of the imidazole moiety (described later). The O^{δ} atom of Cso50 (single-oxidation form of C_p50) forms a hydrogen bond with Thr-47, which is invariant in Prx proteins. We observed a water molecule near the hydroxyl group of the hypervalent intermediate (WAT 1 in Fig. 3). This water molecule might have been released from the hydrogen peroxide after an attack by the thiolate to form the sulfurane-like intermediate.

Reaction Mechanism. From the extensive structural determinations, we propose the reaction mechanism of the C_p oxidation (Fig. 4). In the reduced state, the C_p side chain interacts with Arg-126, which is invariant in all known Prxs (Fig. 4 *a* and *d*). With the addition of hydrogen peroxide, the conformation around the C_p changes so that Arg-126 swings away and His-42 moves near to C_p50, whereas the side chain of C_p50 is still reduced (preoxidation form, Fig. 4*b* and Fig. S1*d*). Then, the sulfur atom nucleophilically attacks one of the oxygen atoms of H_2O_2 from the direction of the energetically low-lying O–O σ^* orbital (Fig. 4*e*). The nucleophilic S–O bond formation would be

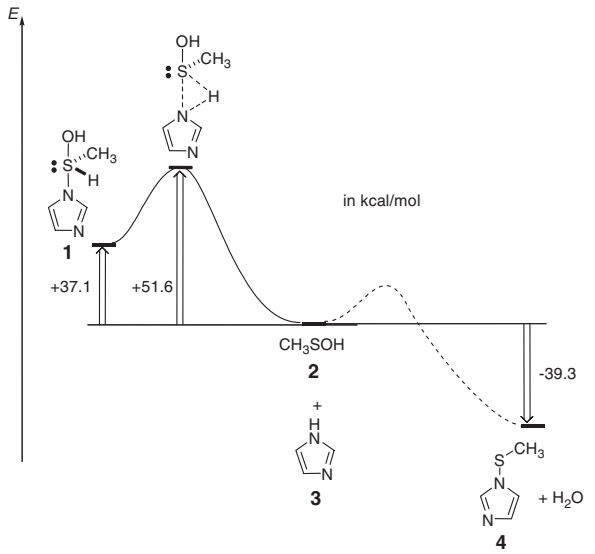

Fig. 5. Reaction coordinate diagram for a model reaction. Shown is the reaction coordinate diagram for the model reaction of methanesulfenic acid (**2**) with imidazole (**3**), which mimics the reaction of cysteine sulfenic acid with imidazole. A solid line shows a reaction path to the sulfurane derivative (hydroxy-imidazolyl-λ^4-sulfanyl)methane (**1**), and a dotted line shows a possible path for the formation of imidazole-1-sulfenic acid (**4**) and H_2O. For the reaction to the sulfurane derivative, the transition state was found at the B3LYP/6–31G* level of theory.

assisted by the nitrogen atom of His-42 to produce the hypervalent sulfur intermediate that contains the $N^{\delta 1}$–S^{γ} covalent bond. Thus, the electron movement from the sulfur to the O–O σ^* orbital of H_2O_2 is compensated by the imidazole nitrogen from the opposite side (Fig. 4*e*). It is noteworthy that in the preoxidation state, the conformation has changed, causing His-42 to move closer to the sulfur atom of C_p50, but the thiol has not been oxidized yet (Fig. 4*b*, Fig. S1*d*). Therefore, it is unreasonable that the $N^{\delta 1}$–S^{γ} covalent bond forms after the oxidation of the sulfur. The hypervalent sulfur intermediate (Fig. 4 *c* and *d*) proceeds by either of the two following different pathways: the peroxidase process or the overoxidation process. This study provides the structural information of the latter process (Fig. S1 *f* and *g*). The hypervalent sulfur intermediate is cleaved into cysteine sulfenic acid and histidine after protonation of the imidazole moiety (Fig. 4*e*), which would be contributed by Arg-149 (Fig. 3). This step was supported by the calculation of the potential energy (described later). The cysteine sulfenic acid proceeds to the overoxidation process with additional hydrogen peroxide molecules. In the sulfinic acid form, the interaction between Arg-126 and Glu-53 remains (Fig. S3). In the sulfonic acid form, the side chain of Arg-126 is rotated toward the C_p50 side chain instead of Glu-53, and so is like the reduced form (Fig. S3).

Energy Calculation of Reaction Intermediates. We proposed the reaction scheme shown in Fig. 4*e*. Here, we describe a calculation supporting the proposal that the hypervalent intermediate is formed as the first step of the oxidation of ApTPx. Because the reaction between cysteine sulfenic acid and histidine could be assumed to form the hypervalent intermediate, we simulated the potential energy along with the possible reaction pathway. The calculation was performed with the models methanesulfenic acid (Fig. 5, **2**) and imidazole (Fig. 5, **3**), which mimic Cys-SOH and His, respectively. The result showed that, with the attack of imidazole nitrogen on the sulfur atom, the hydroxyl group was likely to be eliminated to form imidazole-1-sulfenic acid (Fig. 5, **4**) rather than the formation of (hydroxy-imidazolyl-λ^4-sulfanyl)methane (Fig. 5, **1**). Instead, the cleavage of the hypervalent intermediate to form cysteine sulfenic acid and histidine was found to be reasonable in terms of the potential energy (Fig. 5). These data support the reaction scheme that the hypervalent intermediate is formed before the dissociation to form cysteine sulfenic acid.

Implications for the Hypervalent Intermediate. Cysteine sulfenic acid, a common single-oxidation intermediate of thiol oxidation in proteins, is followed either by conversion to the disulfide or by oxidation to sulfinic acid (double-oxidation state) (24). The stability of the sulfenic acid form is crucial in the overall function of Prx, because this single-oxidation state is a turning point of the two pathways. We propose that the unique $N^{\delta 1}$–S^{γ} covalent bond stabilizes the sulfenic acid-like form against overoxidation in ApTPx, because the hypervalency makes the sulfur atom more positive. The positive charge should retard the electrophilic overoxidation at the sulfur atom. In the case of a human Prx (hORF6), the single-oxidation form has an atomic configuration analogous to, but distinct from, the hypervalent sulfur form of ApTPx; the cysteine sulfenic acid form of C_p47 is stabilized by a hydrogen bond with the His-39 side chain rather than by a covalent bond (14). However, it should be noted that such an atomic configuration is not a common architecture of C_p-SOH in Prx, because the histidine residue (His-39 in hORF6 and His-42 in ApTPx) is not conserved in all Prxs. The mechanism to protect Cys-SOH from undesirable oxidation involves the conversion to other forms in the same oxidation state. Such a mechanism is known in protein tyrosine phosphatase 1B, which involves the conversion of sulfenic acid to the sulfenyl-amide intermediate containing a covalent bond between S^{γ} of the redox active cysteine and the main chain N atom of the nascent residue (25, 26). In ApTPx, however, we propose the mechanism that the formation of the hypervalent sulfur intermediate precedes the appearance of sulfenic acid (Fig. 4*e*). The architecture of the single-oxidation state, the hypervalent sulfur intermediate, is of great importance regarding the selection of the pathways of Prx, namely the peroxidase process or the overoxidation process.

This study shows that sulfurane is involved in a biochemical reaction. In general, sulfurane exists stably when more electronegative atoms are ligated at the apical positions of the sulfur atom. The hypervalent sulfur intermediate of ApTPx adopts this architecture; the two apical positions are occupied by nitrogen (N^{δ} of His-42) and oxygen (O^{δ} of C_p50) atoms. Hypervalent compounds have been studied in the field of organic synthetic chemistry for ≈50 years. Nowadays, hypervalent compounds are known as active reagents such as the Wittig reagent, a hypervalent phosphorus compound. This study expands the importance of hypervalent compounds with respect to the field of biochemistry by demonstrating that a sulfurane derivative occupies a crucial position in biochemical processes. The architecture of hypervalent sulfur in proteins will provide useful guidelines for methodological studies toward the synthesis of hypervalent compounds.

Materials and Methods

Structure Determination. The C207S mutant of ApTPx was purified as described in ref. 21 and was used throughout this study. The crystallization and H_2O_2-mediated oxidation of ApTPx were performed as described in *SI Text, Methods*. Diffraction data were collected at BL41XU and BL38B1 (SPring-8, Japan) in a nitrogen gas stream (100 K) and processed with HKL2000 (27). Structural refinement was performed with REFMAC in the CCP4 suite (28). For the

hypervalent sulfur form, the sulfurane moiety was refined by using the omit map in which His-42 and Cys-50 were removed from the structure factor calculation until late in the refinement. The data collection and refinement statistics are presented in Table S1.

Theoretical Calculation. Geometry optimizations were performed at the RB3LYP (29, 30) level of theory with the 6–31G(d) (31) basis set. The geometry of the stationary point was located and the vibrational analysis was performed with the Gaussian 03 suite of programs (32).

ACKNOWLEDGMENTS. This work was supported in part by the National Project on Protein Structural and Functional Analyses and by a Grant-in-Aid from the Ministry of Education, Science, Sports and Culture. The x-ray diffraction studies were carried out with the approval of the Japan Synchrotron Radiation Research Institute.

1. Musher JI (1969) The chemistry of hypervalent molecules. *Angew Chem Int Ed Engl* 8:54–68.
2. Drabowicz J (1999) Chemistry of hypervalent compounds. *Hypervalent Sulfuranes*, ed. Akiba KY (Wiley-VCH, Weinheim, Germany), pp 211–240.
3. Wood ZA, Schröder E, Robin Harris J, Poole LB (2003) Structure, mechanism and regulation of peroxiredoxins. *Trends Biochem Sci* 28:32–40.
4. Hofmann B, Hecht HJ, Flohe L (2002) Peroxiredoxins. *Biol Chem* 383:347–364.
5. Rhee SG, Kang SW, Chang TS, Jeong W, Kim K (2001) Peroxiredoxin, a novel family of peroxidases. *IUBMB Life* 52:35–41.
6. Denu JM, Tanner KG (1998) Specific and reversible inactivation of protein tyrosine phosphatases by hydrogen peroxide: Evidence for a sulfenic acid intermediate and implications for redox regulation. *Biochemistry* 37:5633–5642.
7. Lee SR, *et al.* (2002) Reversible inactivation of the tumor suppressor PTEN by H_2O_2. *J Biol Chem* 277:20336–20342.
8. Rhee SG, Kang SW, Jeong W, Chang TS, Yang KS, Woo HA (2005) Intracellular messenger function of hydrogen peroxide and its regulation by peroxiredoxins. *Curr Opin Cell Biol* 17:183–189.
9. Allison WS (1976) Formation and reactions of sulfenic acids in proteins. *Acc Chem Res* 9:293–299.
10. Kice JL (1980) Mechanism and reactivity in reactions of organic oxyacids of sulfur and their anhydrides. *Adv Phys Org Chem* 17:65–181.
11. Hogg DR (1990) Chemistry of sulphenic acids and esters. *The Chemistry of Sulfenic Acids and their Derivatives*, ed. Patai S (Wiley, New York), pp 361–402.
12. Claiborne A, *et al.* (1999) Protein-sulfenic acids: Diverse roles for an unlikely player in enzyme catalysis and redox regulation. *Biochemistry* 38:15407–15416.
13. Biteau B, Labarre J, Toledano MB (2003) ATP-dependent reduction of cysteine-sulphinic acid by S. cerevisiae sulphiredoxin. *Nature* 425:980–984.
14. Choi HJ, Kang SW, Yang CH, Rhee SG, Ryu SE (1998) Crystal structure of a novel human peroxidase enzyme at 2.0 Å resolution. *Nat Struct Biol* 5:400–406.
15. Li S, *et al.* (2005) Crystal structure of AhpE from Mycobacterium tuberculosis, a 1-Cys peroxiredoxin. *J Mol Biol* 346:1035–1046.
16. Schröder E, *et al.* (2000) Crystal structure of decameric 2-Cys peroxiredoxin from human erythrocytes at 1.7 Å resolution. *Struct Fold Des* 8:605–615.
17. Sarma GN, *et al.* (2005) Crystal structure of a novel Plasmodium falciparum 1-Cys peroxiredoxin. *J Mol Biol* 346:1021–1034.
18. Mizohata E, *et al.* (2005) Crystal structure of an archaeal peroxiredoxin from the aerobic hyperthermophilic crenarchaeon Aeropyrum pernix K1. *J Mol Biol* 354:317–329.
19. Nakamura T, *et al.* (2006) Crystal structure of thioredoxin peroxidase from aerobic hyperthermophilic archaeon Aeropyrum pernix K1. *Proteins* 62:822–826.
20. Jeon SJ, Ishikawa K (2003) Characterization of novel hexadecameric thioredoxin peroxidase from Aeropyrum pernix K1. *J Biol Chem* 278:24174–24180.
21. Nakamura T, *et al.* (2005) Crystallization and preliminary X-ray diffraction analysis of thioredoxin peroxidase from the aerobic hyperthermophilic archaeon Aeropyrum pernix K1. *Acta Crystallogr F* 61:323–325.
22. Raftery MJ, Yang Z, Valenzuela SM, Geczy CL (2001) Novel intra- and inter-molecular sulfinamide bonds in S100A8 produced by hypochlorite oxidation. *J Biol Chem* 276:33393–33401.
23. Fu X, Mueller DM, Heinecke JW (2002) Generation of intramolecular and intermolecular sulfenamides, sulfinamides, and sulfonamides by hypochlorous acid: A potential pathway for oxidative cross-linking of low-density lipoprotein by myeloperoxidase. *Biochemistry* 41:1293–1301.
24. Barford D (2004) The role of cysteine residues as redox-sensitive regulatory switches. *Curr Opin Struct Biol* 14:679–686.
25. Salmeen A, *et al.* (2003) Redox regulation of protein tyrosine phosphatase 1B involves a sulphenyl-amide intermediate. *Nature* 423:769–773.
26. van Montfort RL, Congreve M, Tisi D, Carr R, Jhoti H (2003) Oxidation state of the active-site cysteine in protein tyrosine phosphatase 1B. *Nature* 423:773–777.
27. Otwinowski Z, Minor W (1997) Processing of X-ray diffraction data collected in oscillation mode. *Methods Enzymol* 276:307–326.
28. Collaborative Computational Project Number 4 (1994) The CCP4 suite: Programs for protein crystallography. *Acta Crystallogr D* 50:760–763.
29. Becke AD (1993) Density-functional thermochemistry. III. The role of exact exchange. *J Chem Phys* 98:5648–5652.
30. Lee C, Yang W, Parr RG (1988) Development of the Colle-Salvetti correlation-energy formula into a functional of the electron density. *Phys Rev B Condens Matter* 37:785–789.
31. Hariharan PC, Pople JA (1973) The influence of polarization function on molecular orbital hydrogenation energies. *Theor Chim Acta* 28:270–283.
32. Frisch MJ, *et al.* (2004) Gaussian 03 (Gaussian, Inc, Wallingford CT).